Talk presented at 1981
Nuclear Science Symposium, Oct. 21-23
San Francisco, CA

Conf-811012--55
BNL 30620
OG 591
MASTER

Optimization of Microchannel Plate Multipliers for Tracking Minimum-Ionizing Particles

K. Oba* and P. Rehak
Physics Department
Brookhaven National Laboratory, Upton, NY 11973

D. Potter
Serin Physics Laboratory corp?
Rutgers University, Piscataway, New Jersey

BNL--30620

DE82 0?0250

*Permanent address: Hamamatsu TV Co., Ltd., Japan

The submitted manuscript has been authored under contract DE-AC02-76CH00016 with the U.S. Department of Energy. Accordingly, the U.S. Government retains a nonexclusive, royalty-free license to publish or reproduce the published form of this contribution, or allow others to do so, for U.S. Government purposes.

OPTIMIZATION OF MICROCHANNEL PLATE MULTIPLIERS FOR TRACKING MINIMUM IONIZING PARTICLES

K. Oba* and P. Rehak
Physics Department
Brookhaven National Laboratory, Upton, NY 11973

D. Potter
Serin Physics Laboratory
Rutgers University, Piscataway, New Jersey

Abstract

The progress in development of special Microchannel Plates for particle tracking is reported. The requirements of i) high spatial resolution, ii) high density of information and, iii) rate capability were found to be satisfied in a thick Microchannel Plate with a CsI coating operating in a focusing magnetic field. The measurements of the Microchannel Plate detection efficiency, gain and noise are presented for several detectors. The pictures of the passage and interaction of the high energy charged particles inside the detector are shown.

Introduction

There has been a great interest recently in the development of tracking detectors with very high spatial resolution and high rate capabilities. The need for such detectors became apparent with the discovery of particles carrying the new flavor quantum numbers charm and beauty.

The predicted lifetime of new particles requires spatial resolution of a few microns for the direct lifetime measurement or for the particle identification via an observation of the secondary vertex. The expected production cross-sections are so low that in order to collect few events the detector has to perform under high rates up to the MHz region.

The principle of a particle tracking detector consisting of microchannel plates (MCP) and phosphor screen is shown in Fig. 1. A fast charged particle passes through the MCP crossing a large number of channel walls. Along the particle path secondary electrons are emitted into some channels of the MCP and generate avalanches inside the channels. The avalanche process in MCP retains the position information of the primary particle, which is made visible on a phosphoric anode. If the density of secondary electrons produced by the particle passage is sufficiently high, we can see a chain of spots corresponding to a projection of the particle trajectory onto the phosphor screen.

Several features of the MCP[1] make this scheme a suitable candidate for the high resolution tracking detector;[2] i) Small channel diameter (~ 12 μm) allows in principle to achieve the position resolution of rms 5 μm. ii) The intrinsic resolving time of the MCP excited by the charged particle is less than one nanosecond[3], thus the detection at high rates is, in principle, possible. iii) The MCP is "live" so the information from it can be used for the event selection (trigger).

In this paper we describe the way to select MCP parameters to optimize the performance of an MCP-tracking detector. The considered parameters are i) the configuration of MCP, ii) the material of channel walls, iii) the external magnetic field, iv) the electric field applied to the MCP, and v) the electric field between the MCP output and the phosphoric anode. The performance of such a detector is reported and the pictures of the interaction within the detector are shown.

*Permanent address: Hamamatsu TV Co., Ltd., Japan.

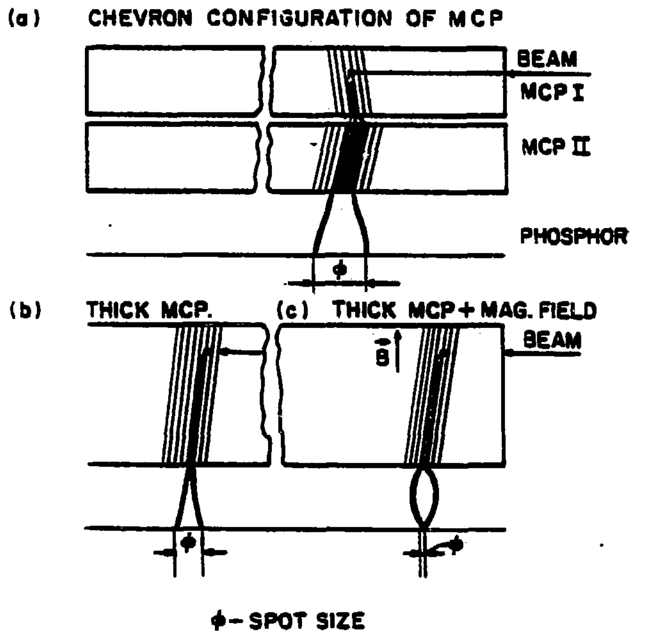

Fig. 1. Principle of the MCP detector for tracking minimum ionizing particles. A beam particle passes through the upper part of the MCP excites some channels along its trajectory. The projection of the particle path is made visible on the phosphoric anode.

Constraints on MCP Tracking Detector

Fig. 1a shows the classical Chevron configuration of MCP used for particle tracking detector. We immediately see a certain loss of the spatial resolution at the interface of MCPI and MCPII. The channels of the second MCP are almost at random position relative to the channels of the first plate and in average, an electron cloud from a single channel of the first MCP spreads to three channels of the second plate[4] resulting in a degradation of the position resolution. To preserve the resolution only one thick MCP is used (Fig. 1b).

The other parameter related to the position resolution is the spot size due to the transverse spread of avalanche electrons arriving at the phosphor screen. The center of the spot retains most of the position information, however, for complicated multiparticle events the small spot size is desirable. Fig. 1c shows the idea of the reduction of the spot size by a magnetic focusing obtained by applying an external magnetic field parallel to the electric field between the MCP and the phosphoric anode.

Additional constraints for the MCP follow from the requirement of the high spot density produced by a minimum ionizing particle crossing the effective thickness of the detector in the upper part of the MCP.

The brightness of different spots on the phosphor screen should be independent of the depth of the particle passage. It means that the MCP should provide about the same amount of the charge at the output - or the MCP should work in a saturated region. In an opposite case of a wide distribution of the spot brightness, the spots at the lower end of the distribution would be lost in a subsequent optical recording (dynamic range limitations) resulting in an apparent decrease of the spot density.

The uniformity of the output charge from an MCP in a saturated region is a result of the electron space charge inside the MCP channel.[1] At sufficiently high charge in the avalanche, the secondary electrons are repulsed back onto the channel wall before they can gain enough energy (from the electric field) to produce additional secondaries at the impact with the wall. The secondary electron yield is reduced to unity and the avalanche reaches the state of dynamic equilibrium propagating down the channel. After exiting from the channel the space charge "blows" electrons apart increasing the spot size. We see that the requirement of uniform spot brightness has an adverse effect on the spot size making the magnetic focusing even more important.

Optimization of the Detector

Magnetic Focusing. Magnetic focusing of electrons in an MCP detector working in the saturation region of the MCP is a direct analogy of a well-known single loop focusing. It is achieved by applying a homogenious magnet field parallel to the acceleration electric field between MCP and the phosphoric anode.

An electron from the electron cloud moving from the output plane of the MCP toward the phosphor screen is subjected to the defocusing action of the electric field produced by all electrons in the cloud. The resulting transverse motion of the electron (in a projection to the plane of the phosphor screen) is similar to the motion of an electron in a magnetron. The electron is accelerated away from the center of the avalanche and as its transverse velocity increases, the electron is subjected to increasing magnetic force which turns the electron back toward the avalanche center. Coming back, the electron moves against the electric field, loses its energy and spends some time close to the center of the electron cloud before it is moved again away from the center.

The time needed for an electron to accomplish one such cycle is mainly a function of the applied magnetic field and depends only weakly on the initial transverse velocity of the electron and on the strength of the defocusing field. If the cycle time of this transverse electron motion is equal to the time of flight of the electron between MCP and the phosphoric anode, the electron reaches the anode while being close to the avalanche center thus minimizing the spot size.

Focusing conditions can be expressed as

$$t_f = t_c \qquad (1)$$

where t_f is the time of flight of electron between MCP-output and phosphor screen and t_c is the above mentioned cycle time.

The real situation is complicated by the spread of initial longitudinal electron energies at the output of the MCP. The electron time of flight thus depends not only on the acceleration potential and on the distance, but also on the longitudinal velocity of electrons exiting the MCP. We can express the electron time of flight spread as a function of the electron initial longitudinal energy spread $\Delta\varepsilon_\ell$

$$|\Delta t_f| \doteq 1/qE \cdot \sqrt{m/2\varepsilon_\ell} \cdot \Delta\varepsilon_\ell \qquad (2)$$

where q - is the electron charge,
E - accelerating field between MCP and phosphor screen,
m - electron mass,
ε_ℓ - initial longitudinal energy.

Formula (2) assumes that $\varepsilon_\ell << q \cdot E \cdot s$ where s is the MCP-phosphor screen distance. We see that in order to minimize the electron time of flight spread (and hence the spot size) the acceleration electric field has to be as strong as possible.

To calculate the transverse motion of electrons, a numerical method is needed. Fig. 2 shows the calculated spot size in μm for the MCP detector as a function of the accelerating voltage for different values of the magnetic field. The assumptions about the MCP avalanche are written on Fig. 2, where $\bar{E}_L$ is the mean initial

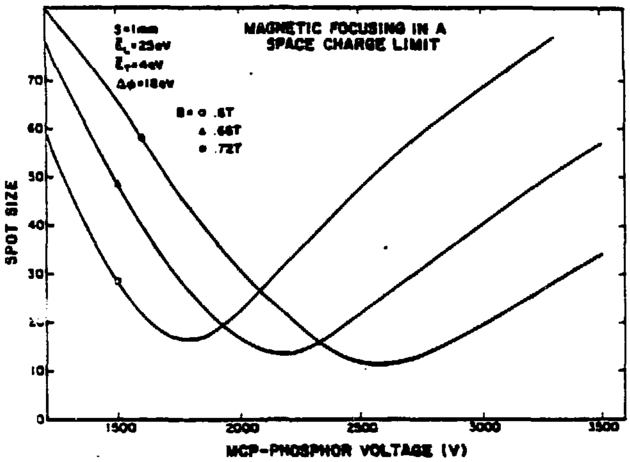

Fig. 2. Calculated spot size in μm as a function of the acceleration field between the output plane of the MCP and the phosphoric anode for different values of the focusing magnetic field. Parameters of the electron avalanche at the MCP output are explained in the text.

longitudinal energy, $\bar{E}_T$ is the mean transverse energy, B the focusing magnetic field and Δφ - (space charge) is the potential difference between the center and the border of a cylindrical electron avalanche exiting the MCP.

The optimal spot size decreases with the magnetic field due to the stronger compression of the transverse electron motion inside the magnetic field.

To obtain the focusing conditions for a different distance between the MCP and the phosphor screen s, the acceleration electric field has to be changed in such a way as to give the same mean electron time of flight. The values of the focusing field for B = .6T are given in Table I below:

s(mm)	E(kV/mm)	V = s·E(kV)
1.3	2.4	3.1
1.5	2.8	4.2
1.7	3.2	5.4

The larger distance s requires the higher acceleration field E and according to formula (2) gives smaller spread in $|\Delta t_z|$ resulting in a smaller spot size. The practical limit for E inside the detector gives the optimal distance s around 1.5 mm.

<u>Single MCP as an Electron Amplifier in a Magnetic Field</u>. The focusing magnetic field of the order of 0.6T is required in the space between the MCP and the phosphor screen. For any practical field configuration it means that the MCP has to perform inside the magnetic field of the same intensity.

Performance of an MCP as an electron amplifier inside the magnetic field was studied in order to determine the optimal bias angle of the MCP.

The Hamamatsu MCP used in the test measured 25 mm in diameter, was 1 mm thick, and had a 0° bias angle. The channel's diameter was 12μ giving length/diameter ratio of about 80.

The anode was connected to the charge sensitive preamplifier followed by a single delay line amplifier with the integrating time τ = 1 μs. The equivalent noise charge (ENC) was about 600 electrons.

Figure 3a shows the most probable gain (peak position) as a function of the magnetic field at different angles between the field and the channel axis. The MCP was excited by UV light and the applied voltage V_{MCP} on the MCP was high enough to obtain a saturated response. We see that the peak position first increases and later decreases with the magnetic field.

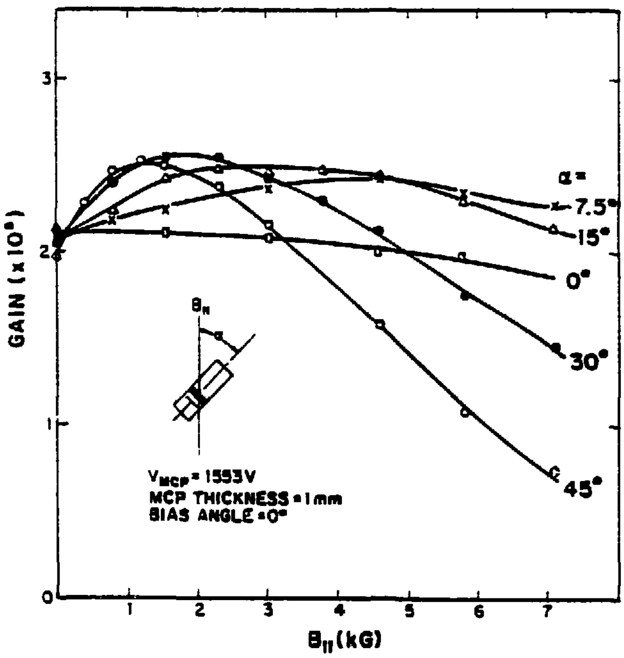

Fig. 3(a). Most probable gain of the single electron response.

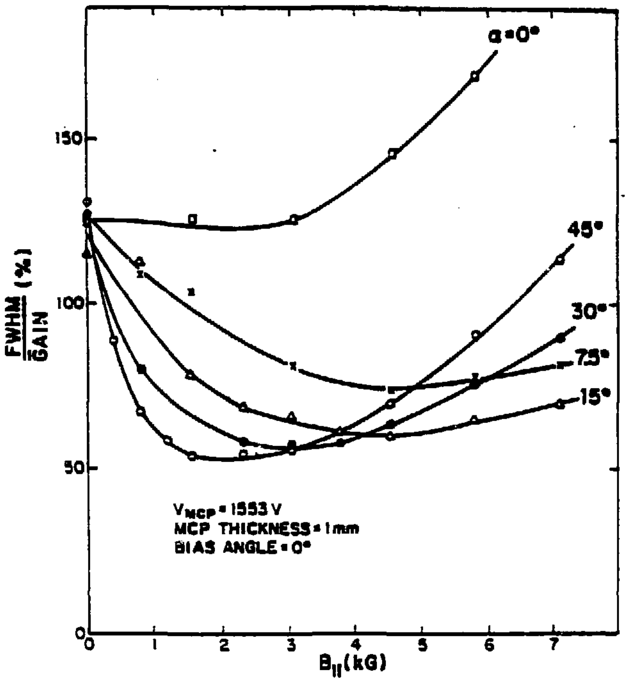

Fig. 3(b). The relative width of the single electron response of the 1 mm thick MCP as a function of the magnetic field for different angles between the channel axis and the direction of the magnetic field.

Figure 3b shows the relative width of the charge distribution FWHM/peak from the same measurement as plotted in Fig. 3a. We see that a 15° angle gives about the best performance for the magnetic field intensity above .5T which is required for focusing.

Distribution of the output charge has a tail corresponding to gain fluctuations toward high values (not shown). The tail which is a consequence of the positive ion feedback became unimportant for the magnetic field above 0.3T at the non zero angle between the magnetic field and the channel axis. The presence of the magnetic field allows us to achieve a saturated gain from a single MCP without the usual problems connected with the positive ion feedback.

We have concluded that an MCP with a 15° angle between the channel and MCP axis (15° bias) should optimize the performance of the MCP as an electron amplifier in the MCP detector.

<u>Study of the Excitation Mechanism of the MCP</u>. The high spot density of the track recorded by MCP detector is particularly desirable for the pattern recognition of the complicated interaction topologies.

The theory of secondary emission[5] predicts that the probability for a particle to excite a channel of the MCP is proportional to the local specific ionization dE/dx. The previous study[2,3] showed the probability of the excitation for a minimum ionizing particle being in a few percent region which results in a density of a few spots per mm for the track inside the MCP.

In this study we have applied a CsI coating inside the channels of the MCP in an attempt to increase the spot density. A CsI coating should increase the spot density by two different processes. First, by its higher secondary electron emission coefficient (at least for low energy electrons); and secondly by acting as a UV-sensitive photocathode inside the channel. A simple straightforward calculation shows that the Cerenkov light emitted by a minimum ionizing particle in the Pb-glass of a MCP into the near UV-region should increase the spot density by a factor of two if the quantum efficiency of the UV light to photoelectron conversion is about 10%.

Figure 4a shows an increase of the MCP efficiency due to the CsI coating. The test was performed at the A-2 test beam at the BNL AGS. The particles (3.5 GeV π^-) passed through MCP under an incident angle of 60°. They crossed relatively few channels in the effective depth of the MCP thus the efficiency gives a direct measure of the excitation probability of MCP channels.

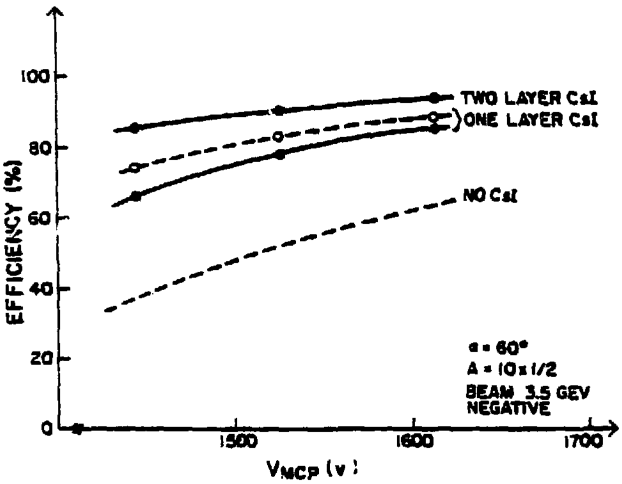

Fig. 4(a). The efficiency of the MCP detector when transversed by a minimum ionizing particle at the angle of 60°. Note the effect of channel coating with CsI.

Figure 4b shows the dependence of the excitation probability (directly related to the spot density) on the kinematics parameter $\eta = P/mc$ of the fast particle. (P is the particle momentum, m the particle mass, and c is the speed of light.) The shape of the probability curve follows a well-known dE/dx curve showing that the Cerenkov light does not contribute appreciable to the excitation process of the MCP. (The Cerenkov light has a threshold at about $\eta = .8$ and rises sharply at that value.)

<u>Performance of the MCP Detector</u>

Based on the studies described in the preceding section, two single stage MCP-detectors were produced by Hamamatsu. Both detectors had the MCP's 1 mm thick, bias angle 15°, channel diameter 12 μ, phosphor P-11 and MCP-phosphoric anode distance 1 mm. One detector used a standard MCP, the second had channels coated with CsI.

The test was performed at the M1-beam at Fermilab. To record the images we used an optical system consisting of a lens, a gated four-stage magnetically focussed image intensifier, which served as an optical switch and an optical amplifier, and a film camera.

The spot size shown in Fig. 5 as a function of

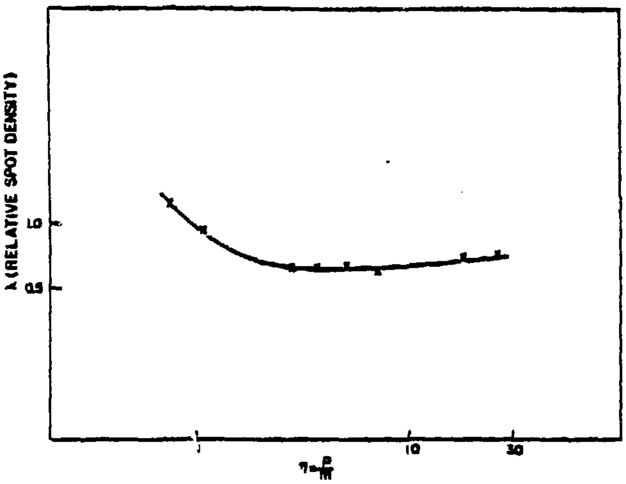

Fig. 4(b). Relative probability of excitation of MCP as a function of $\eta = P/mc$. The probability follows the dE/dx curve showing that the Cerenkov light does not contribute significantly to the excitation process.

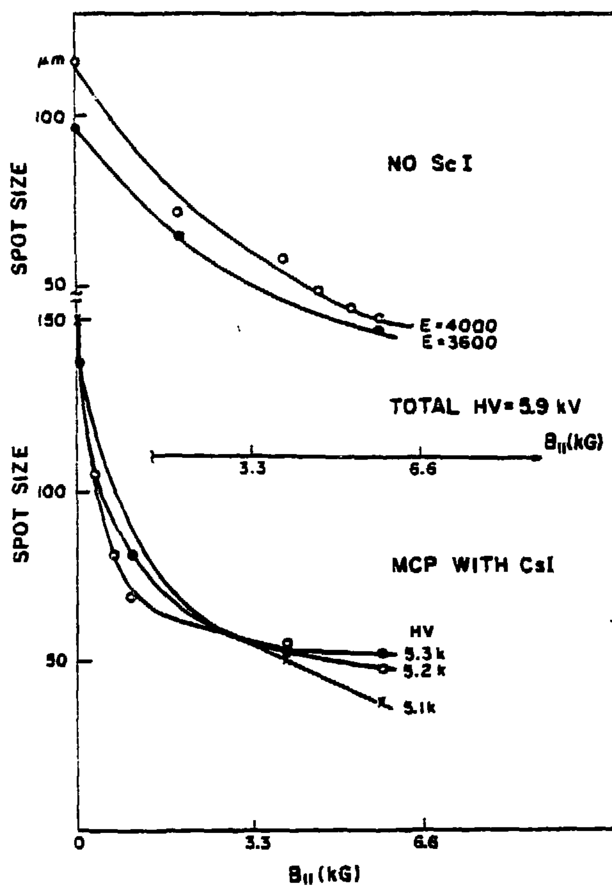

Fig. 5. Measured spot size as a function of the focusing magnetic field for the detector with and without the CsI coating. Electric field of the image intensifier used in the optical system is a parameter of the upper part of Fig. 5.

the focusing magnetic field includes the size degradation (flare) in the used optical image intensifier. If a simpler optical system were used (we do not need an optical amplifier) the spot size would decrease down to 15μ as was measured by a direct photographic recording without the image intensifier. Figures 6a and 6b show the response of detectors as a function of the depth coordinate of the detected particle inside the MCP for the detector without and with the CsI coating, respectively. We see that the CsI layer increases substantially the active depth of the detector.

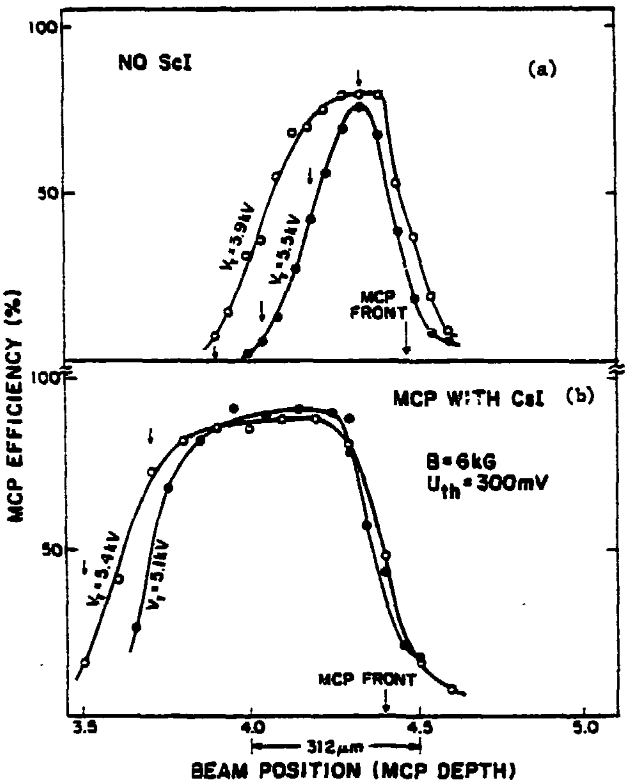

Fig. 6. The efficiency of the MCP detector as a function of the detector depth. (a) detector with no CsI; (b) detector with CsI layer inside the channel. The thickness of the beam defining counters was .2mm.

The examples of the images of 200 GeV/c π^- interactions within the detector are shown in Fig. 7. Examination of a larger sample of photographs provides a measurement of the spot density for the minimum ionizing particles. The measured spot density (2.8 ± .5) spots/mm was essentially the same for both detectors.

The RMS displacement of the dot centers from a least squares fitted line is about 5 μm. This number is a fair estimate of the position resolution of the detectors and is basically limited by the size of the channel.

The excess of dots unrelated to the interactions on Fig. 7 is due to the relatively long decay time of the phosphor of the image intensifier, thus a few spots from previous events were recorded. The intrinsic time resolution of the detector was of the order of 1 μs limited by the decay time of the "P-11" phosphor used at the detector anode.

The rate capability of the detector was estimated from the output charge measurement to be in 10^5/sec region. For some applications an improvement via a lower MCP bleeder resistance may be needed.

Fig. 7. Two examples of the interaction of 200 GeV/c π^- inside the MCP detector. Short blurred tracks are probably due to heavy ionizing nuclear fragments. The incident particle was coming from the bottom.

We would like to especially thank M. Montag for the mechanical design of the focusing magnet and E. Hassel for his technical assistance in the assembly of the magnetic focusing system. We appreciate the patience of the physicists of experiment E-515 during our data taking in the M-1 beam at Fermilab. This research was supported by the U.S. Department of Energy under Contract No. DE-AC02-76CH00016.

References

1. V. Wiza, Nucl. Instr. & Meth. 162, 587 (1979).
2. D.M. Potter, Nucl. Instr. & Meth. 189, 405 (1981).
3. K. Oba, P. Rehak and S.D. Smith, IEEE Trans. Nucl. Sci., NS-28, 705 (1981).
4. E.H. Eberhardt, IEEE Trans. Nucl. Sci., NS-28, 712 (1981).
5. See, e.g., R.E. Simon and B.F. Williams, IEEE Trans. Nucl. Sci., NS-15, 167 (1968).